

**\*\*Volume Title\*\***

*ASP Conference Series, Vol. \*\*Volume Number\*\**

**\*\*Author\*\***

© **\*\*Copyright Year\*\*** *Astronomical Society of the Pacific*

## The many faces of Betelgeuse

Vikram Ravi<sup>1</sup>, Ed Wishnow<sup>1</sup>, Sean Lockwood<sup>1</sup>, Charles Townes<sup>1</sup>

<sup>1</sup>*Space Sciences Laboratory and Department of Physics, University of California, Berkeley, CA 94720, USA*

### Abstract.

The dynamics of the surface and inner atmosphere of the red supergiant star Betelgeuse are the subject of numerous high angular resolution and spectroscopic studies. Here, we present three-telescope interferometric data obtained at  $11.15\,\mu\text{m}$  wavelength with the Berkeley Infrared Spatial Interferometer (ISI), that probe the stellar surface continuum. We find striking variability in the size, effective temperature, and degree of asymmetry of the star over the years 2006–2009. These results may indicate an evolving shell of optically thick material close to the stellar photosphere.

### 1. Introduction

The red supergiant star Betelgeuse ( $\alpha$  Orionis) is a key target for high angular resolution imaging studies at optical and infrared wavelengths because of its large angular diameter ( $\sim 0.047''$ , Michelson & Pease 1921) and high apparent magnitude ( $M_K = -4.38$ ). In recent years, a variety of interferometric campaigns have revealed up to three largely unresolved spots on the stellar surface in various visible, near-infrared and mid-infrared bands (e.g. Wilson et al. 1997; Haubois et al. 2009; Tatebe et al. 2007). These spots range in intensity from a few to a few tens of percent of the total stellar flux. The spots appear to be transient, with stability timescales of less than 8 weeks (Wilson et al. 1997). The properties of these spots have led to a consensus that they indicate large-scale convection cells, as predicted by Schwarzschild (1975).

Numerous puzzles remain regarding the effective temperatures of the spots, and their possible roles in mass loss from Betelgeuse and in shaping the asymmetric inner atmosphere of the star. Imaging studies in the ultraviolet (Gilliland & Dupree 1996) suggest the presence of a plume of material at chromospheric temperatures. Wide-band radio images of Betelgeuse on spatial resolutions of a few stellar radii ( $R_*$ ) also show asymmetry in largely neutral gas at temperatures of a few thousand Kelvin (Lim et al. 1998). A plume at  $6R_*$  was also observed by Kervella et al. (2009), possibly associated with the same gaseous component observed by Lim et al. (1998). Near- and mid-IR spectro-interferometric data for Betelgeuse have been modeled by a variety of authors using a dense shell of molecular gas at temperatures of  $\sim 2000$  K located above a 3600 K photosphere (Perrin et al. 2004), mainly composed of  $\text{H}_2\text{O}$  (Tsuji 2000; Perrin et al. 2007; Ohnaka et al. 2009). This shell, known as a ‘MOLsphere’, is generally thought to lie between  $1.3R_*$  and  $1.5R_*$ , and has been shown to be patchy (Ohnaka et al. 2009). Evidence for MOLspheres is also seen in other stars (e.g. T Lep, Le Bouquin et al. 2009). Betelgeuse is further known to possess an extended dust envelope, with two

shells at angular radii of approximately  $1''$  and  $2''$  (Danchi et al. 1994). A third, newly formed component was found by Bester et al. (1996) at  $0.1''$ . The mechanisms that drive the formation of the dust and shape the dynamic regions close to the surface of Betelgeuse are not well known.

## 2. Observational methods and results

The ISI is a three-telescope interferometer with heterodyne detection systems at each telescope (Wishnow et al., these proceedings; Wishnow et al. 2010). This enables measurements over a narrow bandwidth of  $\sim 5.4$  GHz centered on a given  $\text{CO}_2$  laser local oscillator wavelength. The  $11.15 \mu\text{m}$  wavelength chosen for these measurements corresponds to a region that is free of prominent stellar molecular lines (Weiner et al. 2003b).

Visibilities and closure phases at spatial frequencies between 20–37 SFU<sup>1</sup> were obtained over timespans of a few weeks in each year between 2006 and 2009 (see Table 1 for an observing log). The van Cittert-Zernicke theorem relates the complex cross-correlation between the detected electric fields at different telescopes – the complex visibility – to the two-dimensional Fourier transform of the source brightness distribution. The ISI, like all optical/IR interferometers, however measures the Michelson fringe visibility, which is the power at a given spatial frequency normalized by the total source power. The closure phase is the sum of the fringe phases measured in each of the three baselines. While individual visibility phases vary due to atmospheric turbulence, the closure phase is independent of these variations (Jennison 1958). The spatial frequency sampled by a telescope baseline at a given time is proportional to  $b/\lambda$ , where  $b$  is the baseline length orthogonal to the source direction and  $\lambda$  is the wavelength. By obtaining measurements approximately every five minutes, the ISI samples visibilities and closure phases over a range of spatial frequencies and position angles as the Earth rotates. The telescope configuration used for the measurements reported here was an equilateral triangle with  $\sim 35$  m baseline lengths.

Table 1. Observing log.

Year	Dates (UTC)
2006	8, 9, 10 Nov; 7 Dec
2007	14, 15, 16 Nov
2008	22, 23, 24 Sep
2009	7 Oct; 4, 5, 7, 9, 18, 20, 22 Nov

The visibility and closure phase data for each epoch are shown in Figure 1. The data were calibrated using nightly observations of Aldebaran ( $\alpha$  Tauri), which was assumed to have a diameter of 20 mas and zero closure phase. Data that were affected by systematic errors and poor atmospheric conditions were discarded. The data in each epoch were fit using a simple image model of a centered uniform stellar disk, a point source at an arbitrary location and a large, spherically-symmetric dust shell that did not contribute to the visibility at the sampled spatial frequencies. The fits used a weighted

<sup>1</sup>1 Spatial Frequency Unit (SFU) =  $1 \times 10^5$  cycles/radian.

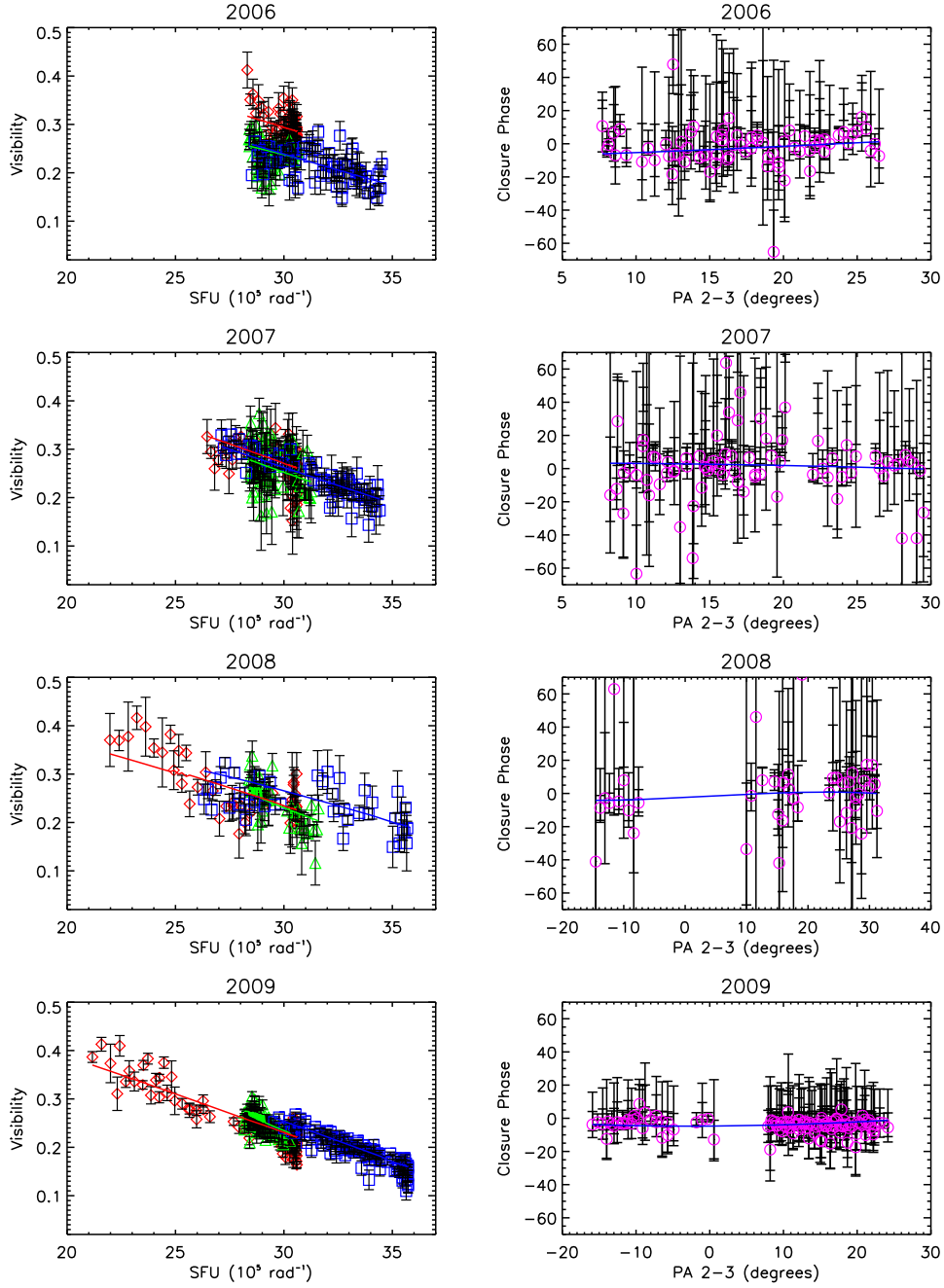


Figure 1. Visibilities (left column) and closure phases (right column) from the 2006, 2007, 2008 and 2009 epochs. Data in red, green and blue (diamonds, triangles and squares respectively) denote telescope baselines 1-2, 2-3 and 3-1, respectively. The closure phases are plotted against the position angle of the 2-3 baseline East of North. The solid lines indicate the best-fit image models.

least-squares minimization technique, with the weights calculated as the inverse squares

of the errors. Each baseline and the closure phase data were weighted equally. For a baseline sampling the two-dimensional spatial frequency plane at a point  $(u, v)$ , the model complex visibility was

$$V(u, v) = \frac{2AJ_1(2\pi r \sqrt{u^2 + v^2})}{2\pi r \sqrt{u^2 + v^2}} + P e^{-2\pi i(ux+vy)}, \quad (1)$$

where  $A$  is the fraction of the total flux contributed by the stellar surface,  $J_1$  denotes a Bessel function of order unity,  $r$  is the stellar angular radius,  $P$  is the fraction of the total flux contributed by the point, and  $x$  and  $y$  are the angular coordinates of the point with respect to the uniform disk center. The fit results are presented in Table 2, with the errors in the last decimal places given in parantheses. The total flux density,  $F_\nu$ , of the star and dust was also estimated for each epoch assuming a flux density of 615 Jy for Aldebaran (Monnier et al. 1998).

Table 2. Fit results.

Year	$A$	$r$ (mas)	$P$	$x$ (mas)	$y$ (mas)	$F_\nu$ ( $10^3$ Jy)
2006	0.51(2)	24.5(8)	0.05(1)	-2.42(1)	-23.70(4)	4.2(2)
2007	0.55(2)	25.7(9)	0.02(1)	-3.25(2)	16.80(8)	4.1(3)
2008	0.47(2)	24.6(8)	0.04(2)	-14.30(3)	12.75(3)	3.8(5)
2009	0.540(5)	25.9(1)	0.013(1)	-24.40(1)	13.92(1)	4.4(1)

Figure 2 shows the best-fit model images for each epoch. The 2006 data were previously analyzed by Tatebe et al. (2007), and despite slightly different techniques used here, the results closely match. We find point sources of varying intensity in each epoch, as well as significant changes in the uniform disk radius of the star. Limb darkening is estimated to reduce the apparent stellar diameter by less than 1% at our wavelength (Bester et al. 1996), and hence was not accounted for.

## 2.1. The effective temperature of the stellar surface

Our absolute measurements of the total flux of Betelgeuse, combined with the fitted stellar size and fraction of the total flux, enable an estimate of the effective temperature of the stellar surface. We used a Planck function, integrated over a 5.4 GHz bandwidth centered on  $11.15 \mu\text{m}$ , to estimate the temperature of the stellar disk. These results are presented in Figure 3. We did not account for extinction caused by the interstellar medium or by intervening layers of dust. However, the interstellar medium and the dust together are expected to attenuate the true stellar flux by only  $\sim 3.1\%$  (Danchi et al. 1994). We also did not account for emission from the dust along the line of sight to the stellar face, again because of the low optical depth.

## 3. Discussion

### 3.1. The source of continuum opacity in the mid-IR

In order to correctly interpret our results, it is crucial to elucidate the nature of the continuum opacity probed in our  $11.15 \mu\text{m}$  observations. This is not an easy task. The

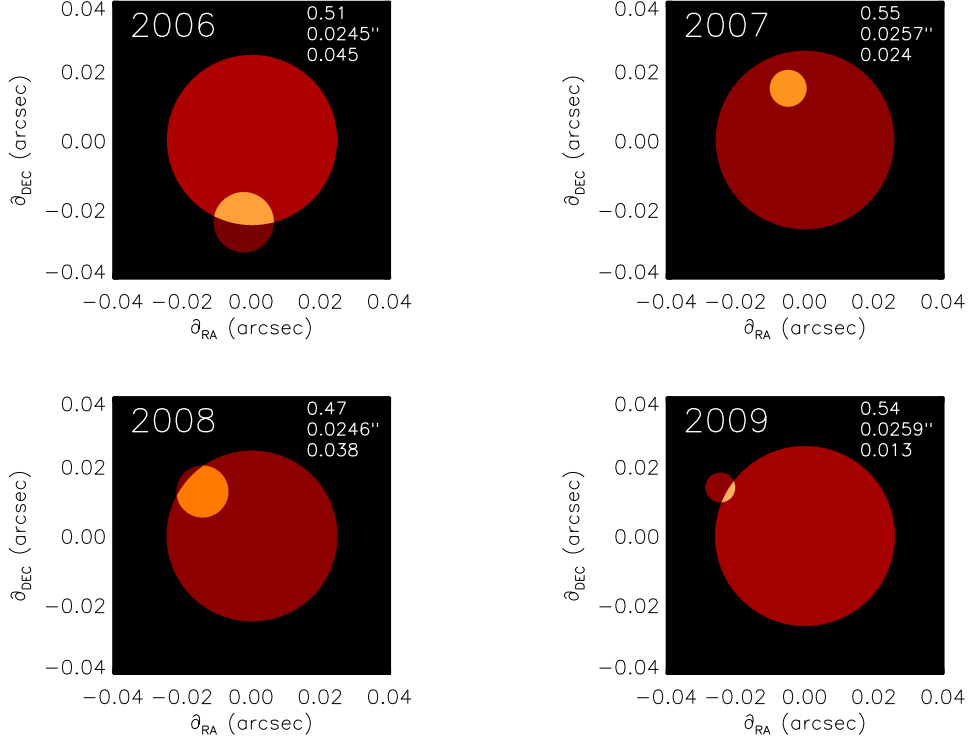


Figure 2. Depictions of the best-fit image models for Betelgeuse during each of the 2006, 2007, 2008 and 2009 epochs. Each figure includes the fit parameters: the fraction of the total flux from the star, the stellar radius in arcseconds, and the fraction of the total flux from the point. The point sources have been given the uniform disk sizes that they would have if they represented regions at a temperature of 7200 K. Our upper limit on the point source diameter is 20 mas.

‘surface’ of a star at a given wavelength can be considered to be the location where the optical depth is unity. The stellar photosphere can be thought of as a surface where the opacity is equivalent to the Rosseland mean opacity, which is a frequency average of the monochromatic opacity. Weiner et al. (2003a) concluded that the mid-IR continuum opacity for solar abundance gas closely matches the Rosseland opacity under the stellar surface conditions present in red supergiant stars. This leads to the implicit conclusion that our  $11.15\ \mu\text{m}$  observations directly probe the stellar photosphere. This conclusion is further supported by the fact that ISI observations in a wavelength band inclusive of a strong  $\text{H}_2\text{O}$  molecular line revealed a larger apparent stellar diameter for the AGB star Mira (*o* Ceti) than that measured at  $11.15\ \mu\text{m}$ . This was indicative of a warm water shell that appeared transparent at  $11.15\ \mu\text{m}$  (Weiner et al. 2003b). Perrin et al. (2007) further show that  $\text{H}_2\text{O}$  molecular lines do not contribute significantly to the  $11.15\ \mu\text{m}$  opacity in their model for the Betelgeuse MOLsphere. We can tentatively conclude that the contribution of a continuum of water lines from a shell above the stellar surface to the  $11.15\ \mu\text{m}$  opacity in Betelgeuse is not significant.

The contribution of the MOLsphere to the  $11.15\ \mu\text{m}$  opacity through means other than water lines cannot however be neglected. Verhoelst et al. (2006) suggested that amorphous alumina ( $\text{Al}_2\text{O}_3$ ) dust in the process of formation in the MOLsphere might

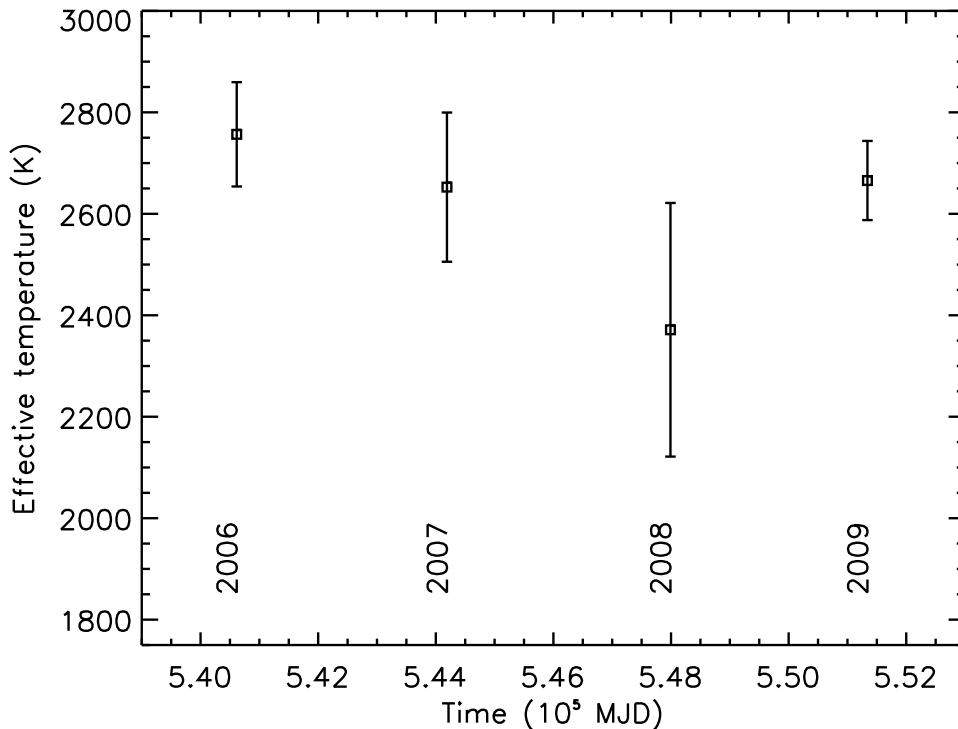


Figure 3. Estimated effective temperatures of the stellar surface of Betelgeuse, neglecting the contribution of any asymmetry, measured over the 2006, 2007, 2008 and 2009 epochs.

contribute to the opacity. Furthermore, Perrin et al. (2007) find, through modeling of spectro-interferometric data in the mid-IR obtained using the VLTI/MIDI instrument, that alumina as well as gaseous SiO appear to contribute to the opacity of the MOL-sphere. At  $11.15\,\mu\text{m}$  wavelength, this model suggests an optical depth of  $\sim 2$ , with the opacity dominated by alumina.

An extension of the ideas of Reid & Menten (1997) for the radio opacity of red supergiant and AGB stars by Tatebe & Townes (2006) shows that electron-hydrogen collisions in thermally ionized inner atmospheres could contribute significantly to the mid-IR opacity. This opacity is proportional to the temperature, naively implying that if a star became hotter, its apparent size would increase. Our present results provide evidence in support of such a phenomenon: the smallest size measurement corresponds to the lowest effective surface temperature (see Table 2 and Figure 3), and the larger size measurements correspond to higher effective surface temperatures.

### 3.2. The origin of the spots

A clear link has been made between spots observed at optical/near-IR wavelengths and the giant convection cell hypothesis of Schwarzschild (1975), as modeled by Chiavassa et al. (2010). However, it is harder to consider the spots we observe in the mid-IR as directly caused by high-temperature regions on the stellar photosphere related to convection cells. The spots seen at 700 nm wavelength by Wilson et al. (1997), which contributed  $\sim 20\%$  of the total flux, were attributed to regions with temperature

excesses of at least 600 K from a mean photospheric temperature of 3600 K. The upper limit on the spot diameters was 15 mas. In contrast, Figure 2 shows that temperatures of at least twice the putative photospheric temperature of 3600 K are in some cases required to produce spots of similar size that are consistent with our mid-IR observations. Such temperatures are inconsistent with the predictions of Schwarzschild (1975) for temperature fluctuations of  $\pm 1000$  K on red giant surfaces.

#### 4. Conclusions and future work

Our present mid-IR continuum results for Betelgeuse show variability in the apparent stellar diameter, location and strength of asymmetries modeled as point sources, and in the effective stellar surface temperature, all on timescales of a year. Intriguingly, we find low effective surface temperatures,  $\sim 1000$  K below those usually associated with the photosphere, and an approximate scaling of the apparent radius with temperature. These results suggest that our measurements are dominated by the behaviour of cool, optically thick material above the stellar photosphere. A possible interpretation of our temperature and size results is that we have witnessed changes in this shell. This interpretation could be extended to explain the systematic decrease in the apparent  $11.15\ \mu\text{m}$  size of Betelgeuse reported by Townes et al. (2009) over the interval 1993–2008. The dominant  $11.15\ \mu\text{m}$  opacity source in the shell could, as suggested by Verhoelst et al. (2006) and Perrin et al. (2007), be alumina dust. If electron-hydrogen collisions, however, dominate the opacity, the apparent size changes could be attributed to temperature changes in largely neutral gas in thermal equilibrium at our measured effective surface temperatures.

Clearly, further work is required to match our observations to radiative transfer models involving layers of material above the stellar photosphere, fully including the various possible opacity sources. More detailed modeling of the closure phase data is also necessary. Our modeled off-center point sources cannot be spots of similar size to those observed at optical/near-IR wavelengths, because the required surface temperatures are unrealistic. The observed asymmetries in our data could possibly indicate large-scale asymmetry in the observed surface.

**Acknowledgments.** W. Fitelson, B. Walp, C.S. Ryan, D.D.S. Hale, K. Tatebe, A.A. Chandler, K. Reichl, R.L. Griffith, V. Toy, as well as many undergraduate researchers all participated in these observations, and their excellent help is greatly appreciated. This research made use of the SIMBAD database. We are grateful for support from the Gordon and Betty Moore Foundation, the Office of Naval Research, and the National Science Foundation.

#### References

- Bester, M., Danchi, W. C., Hale, D., Townes, C. H., Degiacomi, C. G., Mekarnia, D., & Geballe, T. R. 1996, *ApJ*, 463, 336
- Chiavassa, A., Haubois, X., Young, J. S., Plez, B., Josselin, E., Perrin, G., & Freytag, B. 2010, *A&A*, 515, A12+. 1003. 1407
- Danchi, W. C., Bester, M., Degiacomi, C. G., Greenhill, L. J., & Townes, C. H. 1994, *AJ*, 107, 1469
- Gilliland, R. L., & Dupree, A. K. 1996, *ApJ*, 463, L29+

- Haubois, X., Perrin, G., Lacour, S., Verhoelst, T., Meimon, S., Mugnier, L., Thiébaud, E., Berger, J. P., Ridgway, S. T., Monnier, J. D., Millan-Gabet, R., & Traub, W. 2009, *A&A*, 508, 923. [0910.4167](#)
- Jennison, R. C. 1958, *MNRAS*, 118, 276
- Kervella, P., Verhoelst, T., Ridgway, S. T., Perrin, G., Lacour, S., Cami, J., & Haubois, X. 2009, *A&A*, 504, 115. [0907.1843](#)
- Le Bouquin, J., Millour, F., Merand, A., & Vlti Science Operations Team 2009, *The Messenger*, 137, 25
- Lim, J., Carilli, C. L., White, S. M., Beasley, A. J., & Marson, R. G. 1998, *Nat*, 392, 575
- Michelson, A. A., & Pease, F. G. 1921, *ApJ*, 53, 249
- Monnier, J. D., Geballe, T. R., & Danchi, W. C. 1998, *ApJ*, 502, 833. [arXiv:astro-ph/9803027](#)
- Ohnaka, K., Hofmann, K., Benisty, M., Chelli, A., Driebe, T., Millour, F., Petrov, R., Schertl, D., Stee, P., Vakili, F., & Weigelt, G. 2009, *A&A*, 503, 183. [0906.4792](#)
- Perrin, G., Ridgway, S. T., Coudé du Foresto, V., Mennesson, B., Traub, W. A., & Lacasse, M. G. 2004, *A&A*, 418, 675. [arXiv:astro-ph/0402099](#)
- Perrin, G., Verhoelst, T., Ridgway, S. T., Cami, J., Nguyen, Q. N., Chesneau, O., Lopez, B., Leinert, C., & Richichi, A. 2007, *A&A*, 474, 599. [0709.0356](#)
- Reid, M. J., & Menten, K. M. 1997, *ApJ*, 476, 327
- Schwarzschild, M. 1975, *ApJ*, 195, 137
- Tatebe, K., Chandler, A. A., Wishnow, E. H., Hale, D. D. S., & Townes, C. H. 2007, *ApJ*, 670, L21
- Tatebe, K., & Townes, C. H. 2006, *ApJ*, 644, 1145
- Townes, C. H., Wishnow, E. H., Hale, D. D. S., & Walp, B. 2009, *ApJ*, 697, L127
- Tsuji, T. 2000, *ApJ*, 538, 801
- Verhoelst, T., Decin, L., van Malderen, R., Hony, S., Cami, J., Eriksson, K., Perrin, G., Deroo, P., Vandenbussche, B., & Waters, L. B. F. M. 2006, *A&A*, 447, 311. [arXiv:astro-ph/0510486](#)
- Weiner, J., Hale, D. D. S., & Townes, C. H. 2003a, *ApJ*, 589, 976
- 2003b, *ApJ*, 588, 1064
- Wilson, R. W., Dhillon, V. S., & Haniff, C. A. 1997, *MNRAS*, 291, 819
- Wishnow, E. H., Mallard, W., Ravi, V., Lockwood, S., Fitelson, W., Wertheimer, D., & Townes, C. H. 2010, in *Society of Photo-Optical Instrumentation Engineers (SPIE) Conference Series*, vol. 7734 of *Society of Photo-Optical Instrumentation Engineers (SPIE) Conference Series*